JMPM: Jurnal Material dan Proses Manufaktur
Vol. 9, No. 1, p50-62, Juni 2025
DOI: https://doi.org/10.18196/jmpm.v9i1.27238

Effect of Environmental Moisture on Surface Roughness of FDM and SLA Fabricated Components

Muhammad Akhsin Muflikhun[a,1]
[a] Mechanical and Industrial Engineering Department, Universitas Gadjah Mada, Jl. Grafika No. 2, Yogyakarta, 55281, Indonesia
e-mail: akhsin.muflikhun@ugm.ac.id

Correspondence author: akhsin.muflikhun@ugm.ac.id

Keywords:
3D Printing; SLA; FDM; Moisture content; Surface characteristics

ABSTRACT

This study aims to analyze the surface characteristics and moisture contents of three different 3D printed materials, namely Polylactic Acid (PLA) filament, bio-based resin, and standard translucent resin, produced using two distinct manufacturing processes: Fused Deposition Modelling (FDM) for filament materials and Stereolithography (SLA) for resin material. The moisture content was measured using a Moisture Analyzer, and surface characteristics were examined by capturing images through a digital microscope. The results of the moisture content measurement indicated that all three materials exhibited hydrophobic properties with low water content under similar treatments. Among the materials, bio-based resin demonstrated the highest moisture content of 1.53%, followed by translucent resin with 1.26%, and PLA filament with 1.11%. Furthermore, a correlation between applied temperature and moisture content was observed, with translucent resin showing the most stable results, consistently increasing with higher temperatures. In contrast, bio-based resin and PLA filament exhibited unstable behaviours. Surface observation using surface roughness and the digital microscope revealed distinct patterns for the two manufacturing processes. For resin specimens, defects on the surface were evident at lower temperatures and increased with rising temperature. In contrast, PLA filament demonstrated a different surface change pattern, characterized by material melting, leading to a smoother surface. In conclusion, this study sheds light on the surface characteristics and moisture content of 3D printed materials produced through different manufacturing processes. The findings highlight the importance of material selection and processing parameters in achieving desired material properties for various applications in 3D printing.

1. INTRODUCTION

Charles Hull initiated 3D printing commercialization in 1980, these techniques have rapidly developed [1]. 3D printing, also known as Rapid Prototyping (RP) or Additive Manufacturing (AM), involves the addition of thick layers of material to a 3D model to produce the desired object of which a computer controls the process [2]–[4]. A Computer-Aided Design (CAD) model is created using CAD software, and the output is saved in a Stereolithography Language (STL) file format [5], [6]. Then, the 3D model is converted into a series of thin layers by a slicer, and it is used to create a G-code file containing instructions for a specific 3D printer. Slicer software allows the model to be internally optimized with parameters such as printing orientation, infill density, and infill pattern adjustment. These parameters contribute to the properties of a 3D-printed product [7]–[9]. Nowadays, 3D printing is widely used in several fields of human activity [10], [11], such as in aerospace [12], [13], Industrial components [14], [15], automotive parts [16], electronics [17], medical equipment [18], outdoor equipment [19], construction [20], musical instrument [21], and many others. As a versatile stage of technology, 3D printing offers innovative benefits such as improved production efficiency and cost reduction, less waste generation, and high precision creation of complex shapes [22]–[24]. A wide range of materials can be printed with 3D printing, including ceramics, metals, polymers, their composites, and functionally Graded Materials (FGMs) [2], [25], [26]. Based on

ASTM Standard F2792, AM processes are classified into seven groups: directed energy deposition, binding jetting, material jetting, material extrusion, sheet lamination, and vat photopolymerization powder bed fusion [27], [28]. As a result of these seven 3D printing processes, 11 types of 3D printing technology [2]. Fused Deposition Modeling (FDM) and Stereolithography (SLA) printers are the two most popular types of 3D printers on the market [29], [30]. It has been adapted and refined to work on the desktop, making them increasingly more affordable, simpler to use, and more capable [31].

FDM, also known as Fused Filament Fabrication (FFF), belongs to the extrusion material category, which uses an extruder that melts plastic filament to build parts [32], [33]. There are many different types of polymers used in thermoplastics, including; polyurethane (PU) [34], acrylonitrile butadiene styrene (ABS), nylon, polylactic acid (PLA), polycarbonate (PC), polyoxymethylene (POM), high-impact polystyrene (HIPS), polyvinyl alcohol (PVA), polyethylene (PE), polyethylene terephthalate glycol-modified (PETG), and in particular, several chemically and thermally stable materials such as polyether ether ketone (PEEK), polyetherimide (ULTEM), polyphenylsulfone (PPSU), GFRP, and polypropylene (PP) [35]–[37]. On the other hand, an SLA 3D printer uses Ultraviolet (UV) curable resin and a UV light source to make solid objects [38]. Three different UV light sources are typically used, which are Digital Light Processing (DLP) projectors, lasers tuned to a specific wavelength, or Light-Emitting Diodes (LEDs) [32], [39]. Both materials belong to the hydrophobic class, which has a low affinity to water, thus making them water-resistant.

The amount of water in the material must be less than the standard value established during its processing. Recent study, [40] investigated when using PLA and a PLA/polycarbonate blend at high temperatures and humidity. They found significant moisture absorption and hydrolysis, which affected their properties. Previous study [41] demonstrate the performance and effectiveness of four marine structures with varying moisture contents. This includes sodium acetate, fluoropolymers, silicone resins, and silane materials. Results showed that moisture content affected the interaction of materials with concrete and their adhesion inside the pores, reducing their ability to minimize water and chloride penetration. The hydrolytic degradation of polybutylene succinate (PBS), polybutylene adipate-co-terephthalate (PBAT), and PBS/PBAT blend were investigated [42]. The results showed that mechanical properties significantly declined after hydrolysis. Another study [43] showed an analysis of the formaldehyde emission, contact angle, surface roughness, mechanical, and physical properties of the panels revealed significant differences based on moisture content.

This experiment aims to analyze the effect of moisture content on PLA filament and resin material by observing changes in surface characteristics after applying different treatments. The specimens will be subjected to soaking in distilled water at various time intervals, and the impact on surface characteristics will be analyzed concerning the applied temperature during moisture content measurements.

2. MATERIALS AND METHOD

The three materials used for 3D printed specimens in this study were eSUN PLA filament material with a diameter of 1.75 mm [44], eSUN eResin-PLA-Bio-Photopolymer, and Anycubic Translucent UV Resin. 3D printers used to manufacture these materials were FDM type Creality CR 10s Pro V2 with a 0.4 mm nozzle diameter and SLA type Anycubic Mono X, as shown in Figure 1. The material properties are shown in Table 1.

The CAD model was designed in Autodesk Inventor 2020 student edition. The specimen model was then processed using Cura Ultimaker version 4.8 slicing software for the FDM printer and Photon WorkShop V2.1.24 slicing software for the SLA printer. The model dimensions are shown in Figure 2.

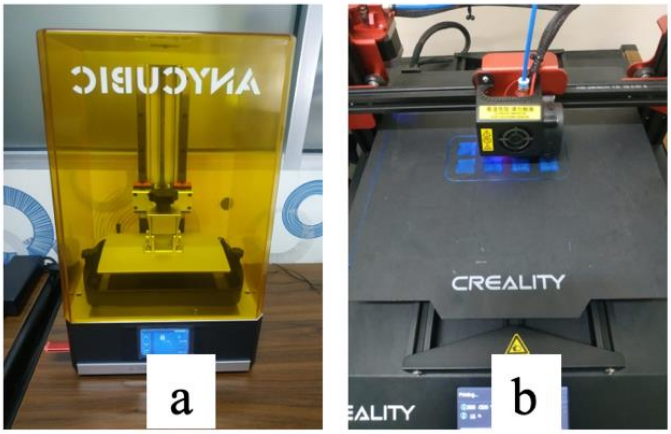

Figure 1. The printing process of the specimens in (a) SLA Anycubic Mono X; (b) FDM CR 10s Pro V2

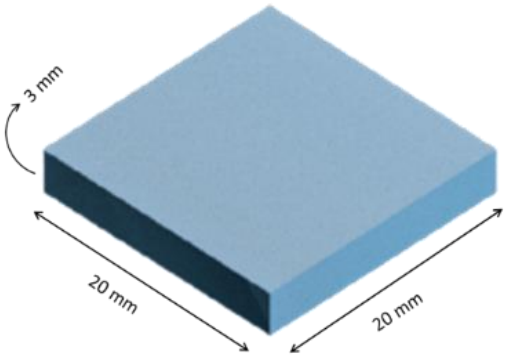

Figure 2. The shape and dimension of the specimen

Table 1. Material Properties

Properties	Unit	eSUN eResin-PLA-Bio-Photopolymer (B)	Anycubic Translucent UV Resin (R)	eSUN PLA Filament (P)
Density	g/m^3	1.07-1.13	1.100 (Liquid) 1.184 (Solid)	1.200-1.250
Viscosity	25°C, MPa. s	200-300	552	-
Hardness	Shore D	75-80	79	
Melting Point	°C	-	-	190-220
Melt Flow Index	g/10min	-	-	7.8
Tensile Yield Strength	MPa	35-50	23.4	62.63
Elongation at Break	%	20-50	14.2	4.43
Flexural Modulus	MPa	40-60	-	65.02
Impact Strength	MPa	-	-	2504.4
Accuracy	kJ/m^2	-	-	4.28

At least twenty samples for each material were prepared. The printing orientation is illustrated in Figure 3. The room temperature was maintained at 25°C to avoid moisture sensitivity during the printing process, which can significantly impact the mechanical properties. The printer setup was the same for all combinations to ensure consistency of the 3D printing results.

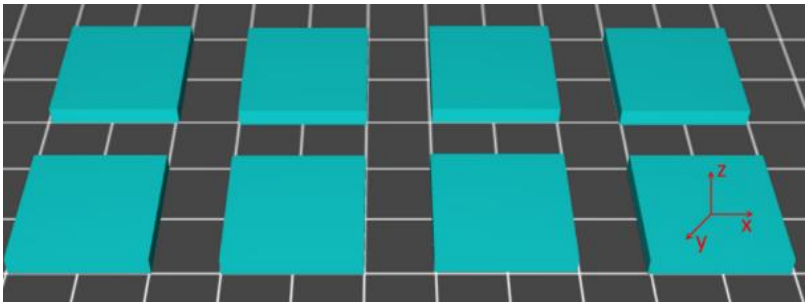

Figure 3. Orientation of the specimens in the printing process

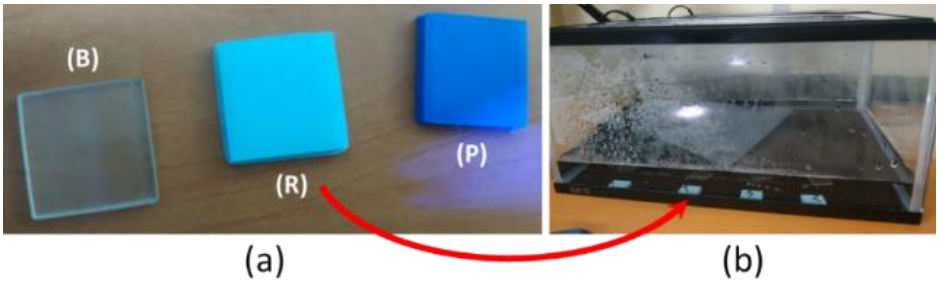

Figure 4. (a) Printed specimen's models (left to right) Anycubic Translucent UV Resin, eSUN eResin-PLA-Bio-Photopolymer, eSUN PLA Filament; (b) the specimen's soaking process

The printed specimen's models are shown in Figure 4. Four different time soaking intervals were used, which are 0 (no soaking), 3, 24, and 72 hours. Specimens of the same soaking time were divided into different heating temperature categories: 105, 125, 145, 165, and 185°C. The configurations of the slicer are listed in Table 2. The printer was leveled once before the printing process to reduce variables. The finished printing model from the SLA printer was soaked in alcohol for 10 minutes and then washed and cleaned for another 10 minutes using distilled water. After that, the specimens were cured using UV light. All models were printed in the same size. The surface characteristics were analyzed concerning the defect area.

Figure 5. Ohaus Moisture Analyzer MB95

A moisture analyzer investigated the moisture content based on the heating method. The moisture content was measured using Ohaus Moisture Analyzer MB95, which determines moisture content using halogen with high 0,001% MC readability. An analysis of continuous records identifies anomalies in water release and the temperature at which those anomalies occurred (e.g., the release of crystallization water or condensation reactions). The specimen was put on the plate and heated up to a specific temperature. The surface characteristics was captured using a digital microscope Dino Capture 2.0 with two kinds of magnification which are 50-60 and 115-125. The surface investigation was done on the specimens before and after the treatments.

Table 2. Slicer configuration in the pre-printing process

Properties	Cura Ultimaker version 4.8	Photon WorkShop V2.1.24
Layer height (mm)	0.2	-
Wall thickness (mm)	0.8	-
Infill pattern (-)	Grid	-
Nozzle temp. (°C)	200	-
Bed temp. (°C)	60	-
Print speed (mm/s)	40	-
Layer thickness (mm)	-	0.050
Normal exposure time (s)	-	2
Off time (s)	-	0.5
Bottom exposure time (s)	-	40
Bottom layers (-)	-	6
Z lift distance (mm)	-	8
Z lift speed (mm/s)	-	2
Z retract speed (mm/s)	-	3

3. RESULTS AND DISCUSSION

3.1 Moisture content

eResin-PLA-Bio-Photopolymer eSUN had the highest moisture content of 1.53%, compared to Anycubic Translucent UV Resin with 1.26%, and eSUN PLA Filament with 1.11%. All specimens belonged to the hydrophobic material category, accounting for the small differences. Graphs revealed several anomalies, particularly for eResin-PLA-Bio-Photopolymer specimens, with mostly stable differences observed in 20 different treatments. However, an anomaly occurred in the results of 24-hour-soaked specimens at 165°C, with the moisture content drastically increasing to 2.48%. The moisture content remained stable at 1.58%, 1.31%, and 1.35% for treatments at temperatures of 105, 125, and 145°C, respectively, as shown in Figure 6.

Anycubic Translucent UV Resin displayed the most stable results among the three types of specimens, with most moisture content increasing with temperature. However, anomalies were observed in the unsoaked specimens, showing a decrease to 0.81% at 165°C. Previous experiences indicated constant increases at temperatures of 105, 125, and 145°C, with the moisture content measured at 0.49%, 0.84%, and 1.14%, respectively, as shown in Figure 7.

eSUN PLA Filament exhibited the most unstable results among the three types of specimens. Anomalous data suggested inconsistencies in moisture content between treatments, particularly for specimens soaked for 3 and 72 hours. For the 3-hour-soaked specimens, the moisture content decreased from 1.11% to 0.5% between temperatures of 105 and 125°C. For the 72-hour-soaked specimens, the value decreased to 0.51% at 165°C from 0.81% at 145°C, as shown in Figure 8.

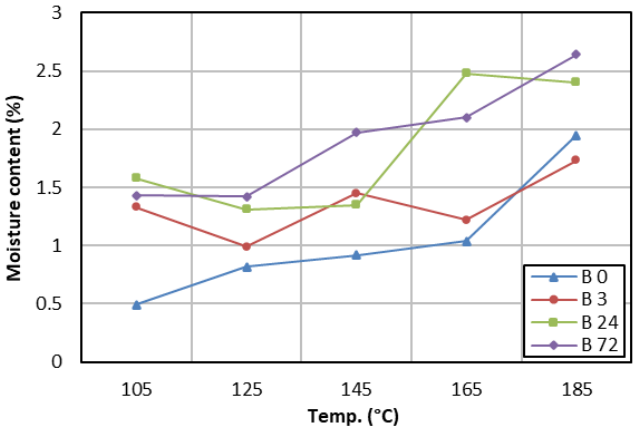

Figure 6. Moisture Analysis for eResin-PLA-Bio-Photopolymer material

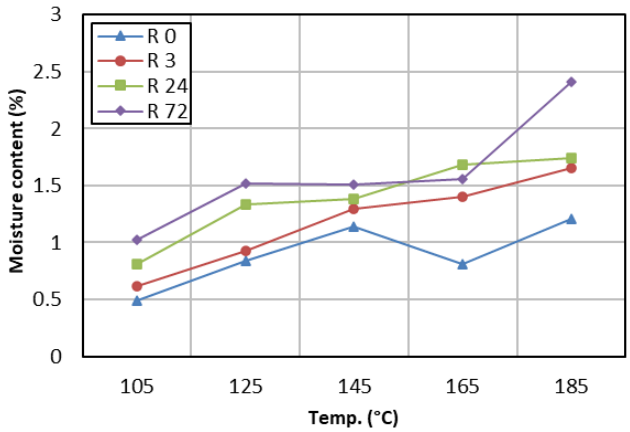

Figure 7. Moisture Analysis for Anycubic Translucent UV Resin material

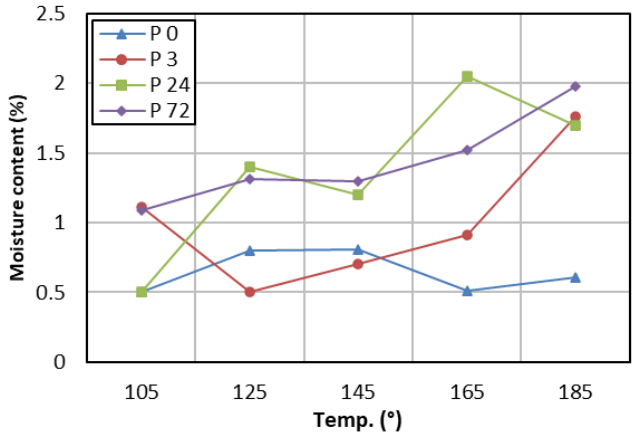

Figure 8. Moisture Analysis for eSUN PLA filament material

The graphs displayed stable results for most specimens, but anomalies were observed in specific conditions. These findings emphasize the significance of material-specific behaviors during 3D printing. The choice of material and its characteristics can significantly influence the quality and properties of 3D-printed products. Understanding these material properties is crucial for optimizing 3D printing processes and achieving desired product outcomes. Further research is needed to investigate the underlying causes of anomalies and develop strategies to improve the reliability and predictability of 3D printing outcomes.

3.2 Surface Characteristics

According to Figure 9 and Figure 10, eSUN eResin-PLA-Bio-Photopolymer and Anycubic Translucent UV Resin specimens at four immersions that were treated with 105, 125, 145, 165, and 185°C heating temperature, respectively, experiencing differences in surface characteristics of which the structural defects getting bigger with raising the temperature. The surface characteristics of both specimens did not change before or after treatment at a temperature of 105°C. Then, at 125°C, 2 out of 4 immersed eResin-PLA-Bio-Photopolymer and Anycubic Translucent UV began to exhibit minor defects, namely, on the test without soaking and soaking for 72 hours. In each temperature increase between 145, 165, and 185°C, structural defects become larger in eResin-PLA-Bio-Photopolymer and Anycubic Translucent UV specimens.

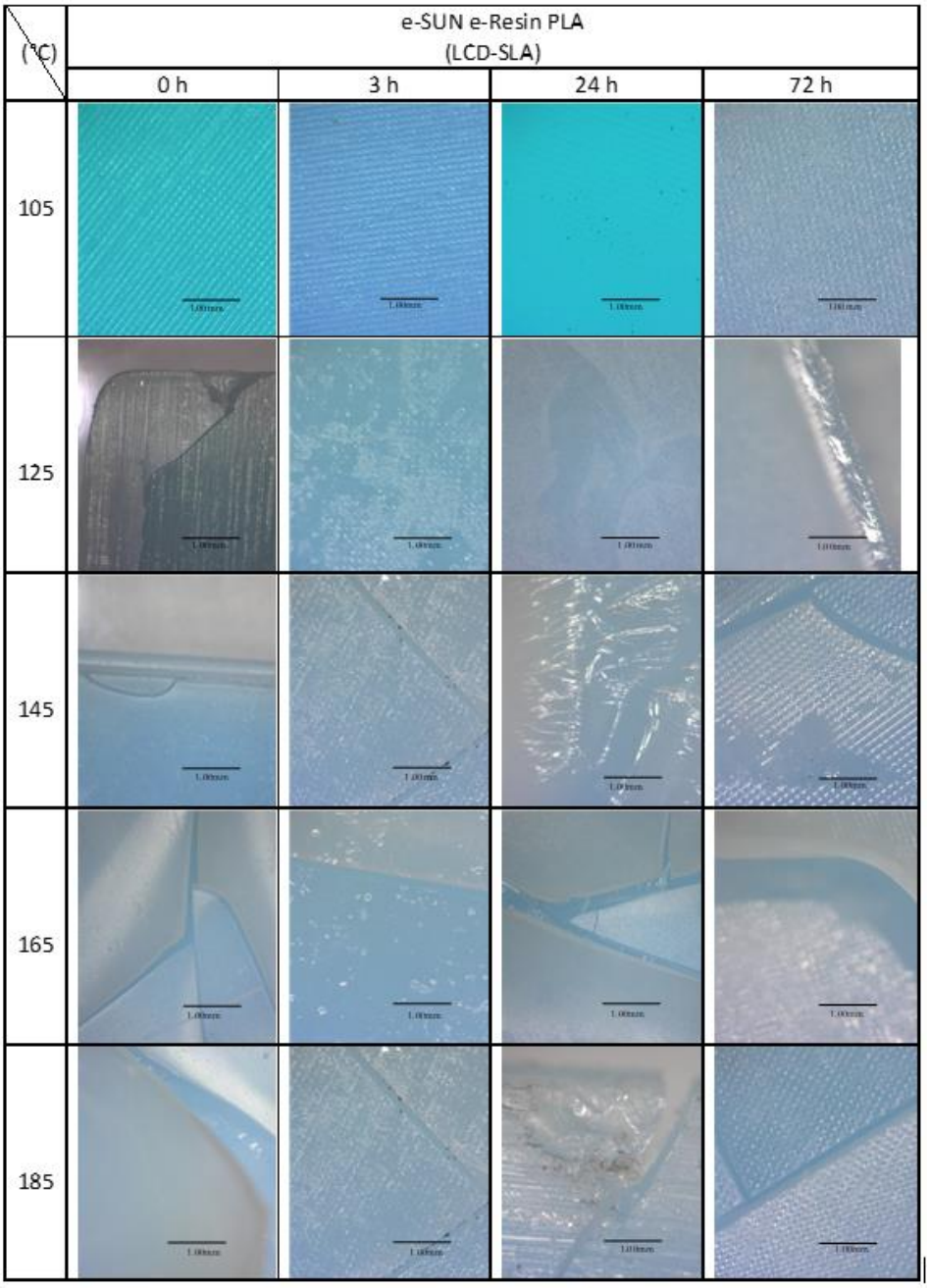

Figure 9. Representative surface characteristics of eSUN e-Resin PLA (LCD-SLA) material after the treatment

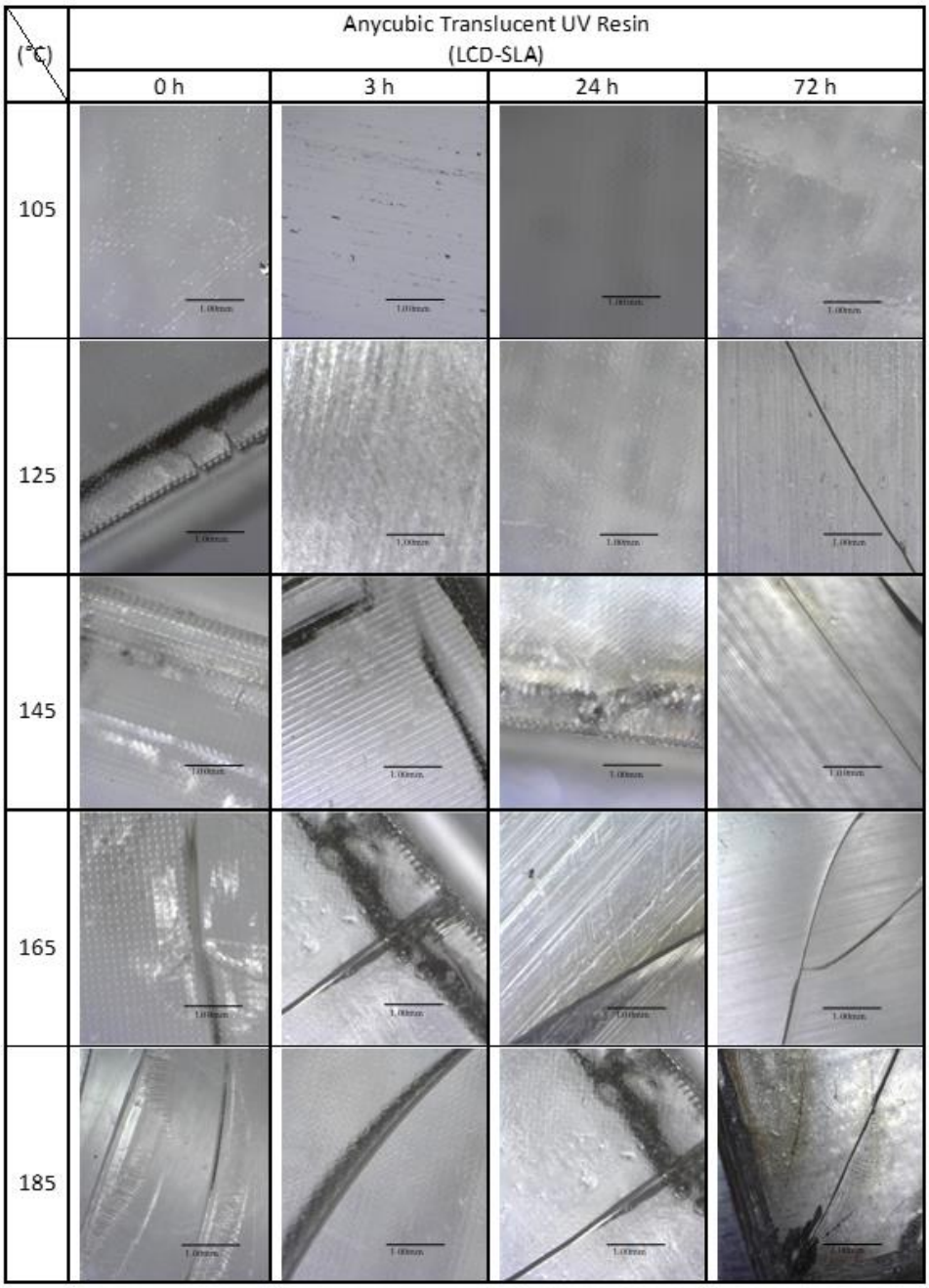

Figure 10. Representative surface characteristics of Anycubic Translucent UV Resin material after the treatments

Compared with the two other types of specimens, as shown in Figure 11, PLA filament specimens did not experience a defect of surface structure (rupture) but melted as the temperature increased. At 105°C, 3 out of 4 soaking treatments curve slightly with an unchanged surface structure. As temperatures increased to 125 and 145°C, all specimens of this material began to curve in a positive z-direction. It is also shown that 1 in 4 treated specimens began to melt slowly, leading to the loss of surface structure. The results also showed that 2 out of 4 treatments encountered surface melting investigated based on surface structures that were not visible anymore, specifically, the unsoaked and 72 hour-soaked specimens. Then, at a temperature of 185°C, all specimens melted on the surface structure characterized by the change of surface structure that turned smooth.

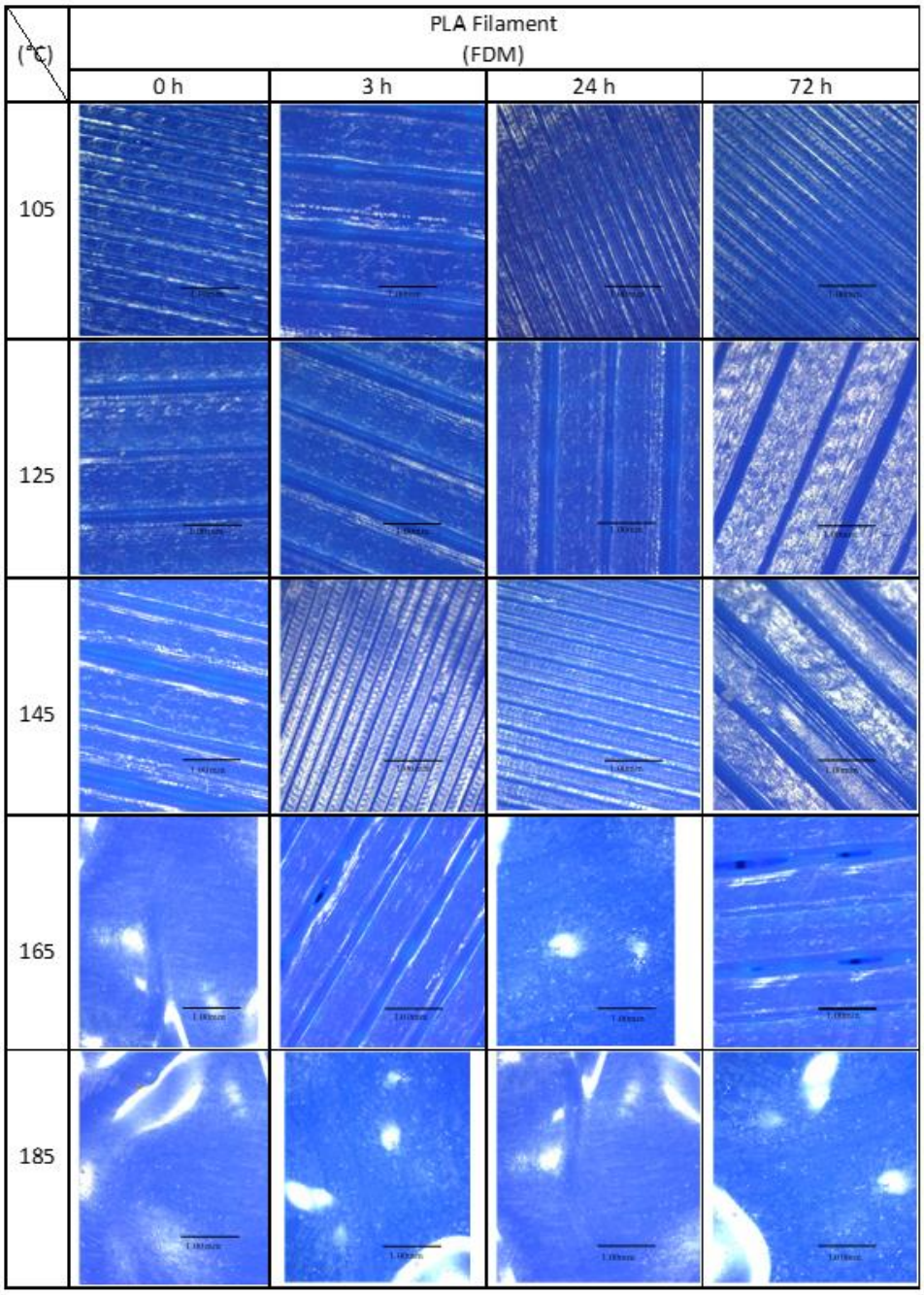

Figure 11. Representative surface characteristics of PLA Filament (FDM) material after the treatments

Therefore, the experiment results show that the melting temperature and heat sensitivity of each material type influenced its surface characteristics [45], [46]. eSUN eResin-PLA-Bio-Photopolymer and Anycubic Translucent UV Resin showed increasing structural defects with rising temperatures, while PLA filament underwent melting and surface smoothing. These findings are essential in 3D printing applications, as they help understand how material properties interact with temperature during the printing process, affecting the quality and integrity of the final printed products. By considering these material-specific behaviors, practitioners can optimize printing parameters and material selection to achieve desired surface characteristics and overall product performance.

As a result of the experiments showing regarding to the moisture content and surface characteristics of eSUN eResin-PLA-Bio-Photopolymer, Anycubic Translucent UV Resin, and PLA filament, when exposed to different treatment temperatures, offer valuable insights when compared to previous studies. Findings align with [40] observations of moisture absorption and hydrolysis in PLA and

PLA/polycarbonate blend at high temperatures and humidity, indicating moisture content variations among materials due to environmental conditions and treatment temperatures. [41] demonstrates the impact of varying moisture contents on material performance, which is evident in the changes observed in surface characteristics as treatment temperatures increased for eResin-PLA-Bio-Photopolymer and Anycubic Translucent UV Resin. The melting and structural changes in PLA filament observed in [42] study indicate temperature-induced degradation, highlighting the importance of considering material-specific behaviors during 3D printing and materials selection. Additionally, [43] analysis of moisture content's effect on various properties of panels aligns with the current experiment's observations, further emphasizing the influence of moisture content on the surface behavior of the tested materials. These insights inform how moisture content and treatment conditions influence the quality and performance of 3D-printed products, highlighting the need for careful consideration during printing to achieve desired outcomes and enhance product performance.

Further characterization was done by using Mitutoyo Surface Roughness SJ-210. Surface roughness test was used to determine the different effects of printing orientation (FDM) and the area exposure of the light (SLA).

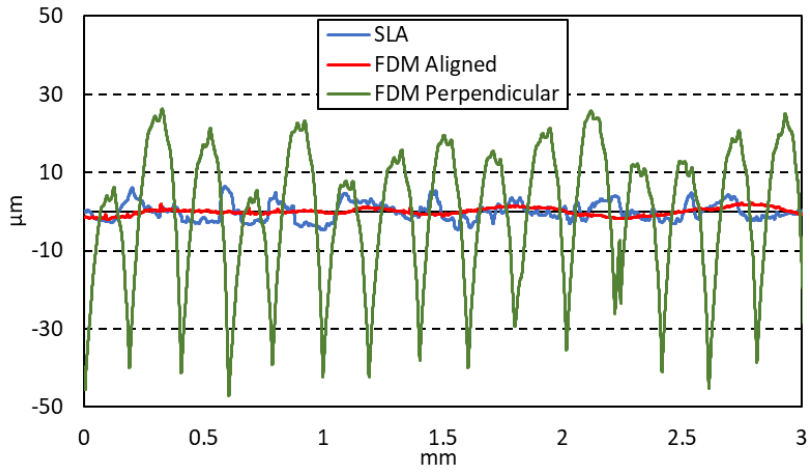

Figure 12. Representative roughness of the different surfaces. (a) SLA roughness, (b) FDM aligned roughness, (c) FDM perpendicular roughness

Fig. 12 shows that the printing direction for SLA (Figure 12 (a)) is less important compared with the FDM. This is due to the printing process of SLA being based on the areas. Since the areas were printed directly, there is less data distribution. This situation did not occur in FDM since the printing process was based on the line trace. Figure 12 (b and c) shows the trend of the surface where the perpendicular roughness showed that peaks and valleys pattern are clearly visible, and flatter roughness from FDM are tracked in the red line. The results of SLA showed that Ra, Rq, and Rz are listed as 1.868 µm, 2.249 µm, and 9.068 µm, respectively. For FDM, the results of RA, Rq, and Rz were 0.730 µm, 0.870 µm, and 3.279 µm for aligned direction, and 14.862 µm, 17.784 µm, 69.976 µm for perpendicular direction, respectively. The surface roughness data showed that the surface conditions are represented by the flatness of the surface and based on the printing methods.

4. CONCLUSION

In this study, we investigated the moisture content and surface characteristics of three materials manufactured using 3D printers of FDM and SLA. The materials tested were eSUN eResin-PLA-Bio-Photopolymer, Anycubic Translucent UV Resin, and eSUN PLA Filament. Our findings revealed several essential conclusions related to the properties of these materials. Firstly, all three materials exhibited hydrophobic behavior, indicating low water content. Among them, eSUN eResin-PLA-Bio-Photopolymer demonstrated the highest moisture content of 1.53%, followed by Anycubic Translucent UV Resin with

1.26% and eSUN PLA Filament with 1.11%. These materials' varying moisture absorption behavior suggests that their composition and characteristics influence their ability to absorb and retain moisture. Furthermore, the moisture content analysis of each specimen resulted in nonlinear data. This nonlinearity can be attributed to the method used in the moisture content analysis, which is based on thermogravimetry analysis (TGA) in the moisture analyzer MB95. Additionally, the analysis might have considered water particles and the content of other elements in the materials. The melting temperature of each material played a significant role in its surface characteristics. In the case of eResin-PLA-Bio-Photopolymer and Anycubic Translucent UV Resin, surface defects were observed at temperatures below higher levels. On the other hand, the PLA filament did not exhibit surface defects but changed structure, melting at a temperature of 165°C. It is showed that the properties of the materials, including their moisture content, composition, and melting temperature, are critical factors influencing their surface characteristics and behavior during exposure to different treatments and temperature conditions. These findings have implications for selecting appropriate materials and optimizing 3D printing processes in various applications. Understanding these material properties is essential to produce high-quality 3D-printed products with desirable surface characteristics and performance. Further research in this area could lead to advancements in 3D printing technology and broaden its applications across multiple industries.

REFERENCES

[1] P. Holzmann, R. J. Breitenecker, A. A. Soomro, and E. J. Schwarz, "User entrepreneur business models in 3D printing," *J. Manuf. Technol. Manag.*, vol. 28, no. 1, pp. 75–94, 2017, doi: 10.1108/JMTM-12-2015-0115.

[2] S. A. M. Tofail, E. P. Koumoulos, A. Bandyopadhyay, S. Bose, L. O'Donoghue, and C. Charitidis, "Additive manufacturing: scientific and technological challenges, market uptake and opportunities," *Mater. Today*, vol. 21, no. 1, pp. 22–37, 2018, doi: 10.1016/j.mattod.2017.07.001.

[3] B. C. Gross, J. L. Erkal, S. Y. Lockwood, C. Chen, and D. M. Spence, "Evaluation of 3D printing and its potential impact on biotechnology and the chemical sciences," *Analytical Chemistry*, vol. 86, no. 7. ACS Publications, pp. 3240–3253, 2014. doi: 10.1021/ac403397r.

[4] ISO/ASTM, "Additive Manufacturing - General Principles Terminology (ASTM52900)," *Rapid Manuf. Assoc.*, vol. 52900, pp. 10–12, 2013, [Online]. Available: http://www.ciri.org.nz/nzrma/technologies.html

[5] K. V. Wong and A. Hernandez, "A Review of Additive Manufacturing," *ISRN Mech. Eng.*, vol. 2012, pp. 1–10, 2012, doi: 10.5402/2012/208760.

[6] B. K. Suryatal, S. S. Sarawade, and S. P. Deshmukh, "Fabrication of medium scale 3D components using a stereolithography system for rapid prototyping," *J. King Saud Univ. - Eng. Sci.*, vol. 35, no. 1, pp. 40–52, 2023, doi: 10.1016/j.jksues.2021.02.012.

[7] R. Patel, C. Desai, S. Kushwah, and M. H. Mangrola, "A review article on FDM process parameters in 3D printing for composite materials," *Mater. Today Proc.*, vol. 60, pp. 2162–2166, 2022, doi: 10.1016/j.matpr.2022.02.385.

[8] J. Fernandes, A. M. Deus, L. Reis, M. F. Vaz, and M. Leite, "Study of the influence of 3D printing parameters on the mechanical properties of PLA," *Proc. Int. Conf. Prog. Addit. Manuf.*, vol. 2018-May, pp. 547–552, 2018, doi: 10.25341/D4988C.

[9] M. M. Hanon, J. Dobos, and L. Zsidai, "The influence of 3D printing process parameters on the mechanical performance of PLA polymer and its correlation with hardness," *Procedia Manuf.*, vol. 54, pp. 244–249, 2020, doi: 10.1016/j.promfg.2021.07.038.

[10] Y. Wang, R. Blache, and X. Xu, "Selection of additive manufacturing processes," *Rapid Prototyp. J.*, vol. 23, no. 2, pp. 434–447, 2017, doi: 10.1108/RPJ-09-2015-0123.

[11] A. V. kumar, "A Review paper on 3D-Printing and Various Processes Used in the 3D-Printing," *Interantional J. Sci. Res. Eng. Manag.*, vol. 06, no. 05, pp. 953–958, 2022, doi: 10.55041/ijsrem13278.

[12] R. Liu, Z. Wang, T. Sparks, F. Liou, and J. Newkirk, "Aerospace applications of laser additive manufacturing," in *Laser Additive Manufacturing: Materials, Design, Technologies, and Applications*, Elsevier, 2017, pp. 351–371. doi: 10.1016/B978-0-08-100433-3.00013-0.

[13] S. C. Joshi and A. A. Sheikh, "3D printing in aerospace and its long-term sustainability," *Virtual Phys. Prototyp.*, vol. 10, no. 4, pp. 175–185, 2015, doi: 10.1080/17452759.2015.1111519.
[14] A. D. Nugraha *et al.*, "First-rate manufacturing process of primary air fan (PAF) coal power plant in Indonesia using laser powder bed fusion (LPBF) technology," *J. Mater. Res. Technol.*, vol. 18, pp. 4075–4088, 2022, doi: 10.1016/j.jmrt.2022.04.056.
[15] C. Buchanan and L. Gardner, "Metal 3D printing in construction: A review of methods, research, applications, opportunities and challenges," *Eng. Struct.*, vol. 180, pp. 332–348, 2019, doi: 10.1016/j.engstruct.2018.11.045.
[16] V. Sreehitha, "Impact of 3D Printing in Automotive Industries," *Int. J. Mech. Prod. Eng.*, vol. 5, no. 5, pp. 2320–2092, 2017, [Online]. Available: http://iraj.in
[17] E. MacDonald *et al.*, "3D printing for the rapid prototyping of structural electronics," *IEEE Access*, vol. 2, pp. 234–242, 2014, doi: 10.1109/ACCESS.2014.2311810.
[18] F. P. W. Melchels, J. Feijen, and D. W. Grijpma, "A review on stereolithography and its applications in biomedical engineering," *Biomaterials*, vol. 31, no. 24, pp. 6121–6130, 2010, doi: 10.1016/j.biomaterials.2010.04.050.
[19] M. A. Muflikhun and D. A. Sentanu, "Characteristics and performance of carabiner remodeling using 3D printing with graded filler and different orientation methods," *Eng. Fail. Anal.*, vol. 130, p. 105795, 2021, doi: 10.1016/j.engfailanal.2021.105795.
[20] M. Sakin and Y. C. Kiroglu, "3D Printing of Buildings: Construction of the Sustainable Houses of the Future by BIM," *Energy Procedia*, vol. 134, pp. 702–711, 2017, doi: 10.1016/j.egypro.2017.09.562.
[21] N. A. S. Alfarisi, G. N. C. Santos, R. Norcahyo, J. Sentanuhady, N. Azizah, and M. A. Muflikhun, "Model optimization and performance evaluation of hand cranked music box base structure manufactured via 3D printing," *Heliyon*, vol. 7, no. 12, p. e08432, 2021, doi: 10.1016/j.heliyon.2021.e08432.
[22] Z. X. Low, Y. T. Chua, B. M. Ray, D. Mattia, I. S. Metcalfe, and D. A. Patterson, "Perspective on 3D printing of separation membranes and comparison to related unconventional fabrication techniques," *J. Memb. Sci.*, vol. 523, pp. 596–613, 2017, doi: 10.1016/j.memsci.2016.10.006.
[23] C. Edwards, "Additive Manufacturing (or 3D Printing)," *Bloom. Encycl. Des.*, pp. 7–8, 2017, doi: 10.5040/9781472596178-bed-a119.
[24] M. Jiménez, L. Romero, I. A. Domínguez, M. D. M. Espinosa, and M. Domínguez, "Additive Manufacturing Technologies: An Overview about 3D Printing Methods and Future Prospects," *Complexity*, vol. 2019, no. 1, p. 9656938, 2019, doi: 10.1155/2019/9656938.
[25] C. Zhu *et al.*, "Highly compressible 3D periodic graphene aerogel microlattices," *Nat. Commun.*, vol. 6, no. 1, p. 6962, 2015, doi: 10.1038/ncomms7962.
[26] S. A. Hussain, M. S. Charoo, and M. I. Ul Haq, "3D printing of functionally graded materials: Overcoming challenges and expanding applications," in *Multi-material Additive Manufacturing: Processing, Properties, Opportunities, and Challenges*, Elsevier, 2025, pp. 67–97. doi: 10.1016/B978-0-443-29228-6.00004-9.
[27] C. Weißenfels, *Additive Manufacturing Processes*, vol. 97. Springer, 2022. doi: 10.1007/978-3-030-87337-0_2.
[28] E. Pei, I. R. Kabir, and B. Leutenecker-Twelsiek, "History of AM," in *Springer Handbooks*, vol. Part F1592, Springer, 2023, pp. 3–29. doi: 10.1007/978-3-031-20752-5_1.
[29] T. N. A. T. Rahim, A. M. Abdullah, and H. Md Akil, "Recent Developments in Fused Deposition Modeling-Based 3D Printing of Polymers and Their Composites," *Polym. Rev.*, vol. 59, no. 4, pp. 589–624, 2019, doi: 10.1080/15583724.2019.1597883.
[30] Z. Liu, Y. Wang, B. Wu, C. Cui, Y. Guo, and C. Yan, "A critical review of fused deposition modeling 3D printing technology in manufacturing polylactic acid parts," *Int. J. Adv. Manuf. Technol.*, vol. 102, no. 9–12, pp. 2877–2889, 2019, doi: 10.1007/s00170-019-03332-x.
[31] J. R. C. Dizon, A. H. Espera Jr, Q. Chen, and R. C. Advincula, "Mechanical characterization of 3D-printed polymers," *Addit. Manuf.*, vol. 20, pp. 44–67, 2018.
[32] T. Finnes and T. Letcher, "High Definition 3D Printing-Comparing SLA and FDM Printing Technologies," *J. Undergrad. Res.*, vol. 13, no. 1, p. 3, 2015.

[33] B. Shaqour *et al.*, "Gaining a better understanding of the extrusion process in fused filament fabrication 3D printing: a review," *Int. J. Adv. Manuf. Technol.*, vol. 114, no. 5–6, pp. 1279–1291, 2021, doi: 10.1007/s00170-021-06918-6.

[34] F. Tanbar *et al.*, "Hybrid lattice structure with micro graphite filler manufactured via additive manufacturing and growth foam polyurethane," *Compos. Part C Open Access*, vol. 15, p. 100516, 2024, doi: 10.1016/j.jcomc.2024.100516.

[35] E. G. Gordeev, A. S. Galushko, and V. P. Ananikov, "Improvement of quality of 3D printed objects by elimination of microscopic structural defects in fused deposition modeling," *PLoS One*, vol. 13, no. 6, p. e0198370, 2018, doi: 10.1371/journal.pone.0198370.

[36] A. J. N. Putro *et al.*, "Optimization of Innovative Hybrid Polylactic Acid+ and Glass Fiber Composites: Mechanical, Physical, and Thermal Evaluation of Woven Glass Fiber Reinforcement in Fused Filament Fabrication 3D Printing," *J. Compos. Sci.*, vol. 9, no. 4, p. 164, 2025, doi: 10.3390/jcs9040164.

[37] A. D. Nugraha *et al.*, "Investigating the mechanical properties and crashworthiness of hybrid PLA/GFRP composites fabricated using FDM-filament winding," *Heliyon*, vol. 10, no. 20, 2024, doi: 10.1016/j.heliyon.2024.e39062.

[38] C. Mendes-Felipe, J. Oliveira, I. Etxebarria, J. L. Vilas-Vilela, and S. Lanceros-Mendez, "State-of-the-Art and Future Challenges of UV Curable Polymer-Based Smart Materials for Printing Technologies," *Adv. Mater. Technol.*, vol. 4, no. 3, p. 1800618, 2019, doi: 10.1002/admt.201800618.

[39] S. Swetha, T. J. Sahiti, G. S. Priya, K. Harshitha, and A. Anil, "Review on digital light processing (DLP) and effect of printing parameters on quality of print," *Interactions*, vol. 245, no. 1, p. 178, 2024, doi: 10.1007/s10751-024-02018-5.

[40] A. M. Harris and E. C. Lee, "Durability of polylactide-based polymer blends for injection-molded applications," *J. Appl. Polym. Sci.*, vol. 128, no. 3, pp. 2136–2144, 2013, doi: 10.1002/app.38407.

[41] M. J. Al-Kheetan, M. M. Rahman, and D. A. Chamberlain, "Fundamental interaction of hydrophobic materials in concrete with different moisture contents in saline environment," *Constr. Build. Mater.*, vol. 207, pp. 122–135, 2019, doi: 10.1016/j.conbuildmat.2019.02.119.

[42] R. Muthuraj, A. Mohanty, and M. Misra, "Hydrolytic degradation of biodegradable polyesters under simulated environmental conditions," *Annu. Tech. Conf. - ANTEC, Conf. Proc.*, vol. 132, no. 27, 2015.

[43] M. Baharoğlu, G. Nemli, B. Sari, S. Bardak, and N. Ayrilmiş, "The influence of moisture content of raw material on the physical and mechanical properties, surface roughness, wettability, and formaldehyde emission of particleboard composite," *Compos. Part B Eng.*, vol. 43, no. 5, pp. 2448–2451, 2012, doi: 10.1016/j.compositesb.2011.10.020.

[44] eSUN, "eSUN PLA+ Technical Data Sheet," no. 6, pp. 3–4, 2021, [Online]. Available: https://www.esun3d.com/uploads/eSUN_PLA+-Filament_TDS_V4.0.pdf

[45] P. Wang, B. Zou, H. Xiao, S. Ding, and C. Huang, "Effects of printing parameters of fused deposition modeling on mechanical properties, surface quality, and microstructure of PEEK," *J. Mater. Process. Technol.*, vol. 271, pp. 62–74, 2019, doi: 10.1016/j.jmatprotec.2019.03.016.

[46] P. Wang, B. Zou, and S. Ding, "Modeling of surface roughness based on heat transfer considering diffusion among deposition filaments for FDM 3D printing heat-resistant resin," *Appl. Therm. Eng.*, vol. 161, p. 114064, 2019, doi: 10.1016/j.applthermaleng.2019.114064.